



Sittakul, V., & Cryan, MJ. (2009). A 2.4-GHz wireless-over-fibre system using photonic active integrated antennas (PhAIAs) and lossless matching circuits. *Journal of Lightwave Technology*, 27(14), 2724 - 2731. <https://doi.org/10.1109/JLT.2009.2015587>

Peer reviewed version

Link to published version (if available):  
[10.1109/JLT.2009.2015587](https://doi.org/10.1109/JLT.2009.2015587)

[Link to publication record in Explore Bristol Research](#)  
PDF-document

## University of Bristol - Explore Bristol Research

### General rights

This document is made available in accordance with publisher policies. Please cite only the published version using the reference above. Full terms of use are available:  
<http://www.bristol.ac.uk/red/research-policy/pure/user-guides/ebr-terms/>

# A 2.4-GHz Wireless-Over-Fibre System Using Photonic Active Integrated Antennas (PhAIAs) and Lossless Matching Circuits

Vitawat Sittakul, *Student Member, IEEE*, and Martin J. Cryan, *Senior Member, IEEE*

**Abstract**—This paper demonstrates that very low cost wireless-over-fibre systems can be implemented without RF amplification by using lossless matching techniques. Single stub matching circuits were designed on low loss substrates and integrated with photodiode chips and results show that the link gain can be theoretically improved by more than 8 dB. A 2-port link gain model is developed using Agilent ADS which allows simple wideband modeling of such systems. Finally the system is tested using a “live” access point both with and without matching and results show that a maximum RF range of 4 m can be obtained at 2 Mbps data rate over 317 m of installed MMF with no RF amplification.

**Index Terms**—Radio-over-fibre, vertical cavity surface emitting lasers (VCSELs), WLAN.

## I. INTRODUCTION

THERE is much interest in wireless-over-fibre (WoF) links operating at 2.4 GHz for the distribution of WiFi signals within buildings, hotels, campuses and airports [1]–[6]. These Distributed Antenna Systems (DASs) often employ high specification lasers and RF amplification in order to achieve good link gain and large RF ranges from remote antenna to the user. However, there are opportunities for very low cost modules with reduced RF ranges giving room-scale coverage of 5–10 m [7], [8]. In [8] a range of 5 m was shown with a carrier frequency of 60 GHz using an electroabsorption modulator (EAM) based scheme which requires no laser at the remote end of the link. However, EAMs are not low cost and can suffer from low responsivity and be polarization sensitive. The approach outlined in [7] shows that low cost vertical cavity surface emitting lasers (VCSELs) can be used within the photonic active integrated antenna (PhAIA) concept [7], [9] which enables integrated modules with no RF amplification to be used at the remote end. The use of VCSELs with low bias current requirements and the removal of RF amplification and associated DC biasing circuitry results in a very low DC power budget, in the order of 10 mW, at the remote end which opens possibilities for DC power-over-fibre operation [10], further reducing implementation costs. In [7] peer-to-peer operation was shown in combination with simple matching based on variation in antenna input

impedance with contact position on the non-radiating edge of the antenna. Here, a number of further developments are presented. First, the noise figure (NF) of different length links is estimated and the link gain of the in-building fibre is measured directly. Second, a lossless matching circuit is designed and implemented for the photodiode to improve the link gain. Finally, live trials using the University of Bristol WiFi network and impedance matched PhAIAs are presented.

Fig. 1 shows the generic scenario under consideration. It is a bidirectional system using two MMF links. The system uses low cost VCSELs and photodiodes (PDs) operating at 850 nm. The wireless router is a dual antenna module, one of which is removed to enable direct coaxial tapping-off of the RF signals. This approach ensures that local users can still access the router. The tapped-off signal is then fed to a coaxial splitter which enables bidirectional operation of the system, albeit with a reduction in link gain due to splitter loss. These losses could be removed or reduced with the use of amplifiers or circulators, however this paper is addressing the very simplest, lowest possible cost scenario as a benchmark. The RF signals are then fed in to the transceiver module consisting of matching circuits and, VCSEL and PD mounted on planar substrates. Low cost fibre alignment fixtures have been used to produce portable units amenable to testing. At the remote end, PhAIA modules are used whereby the optical devices are mounted directly on the backside of 2.4 GHz planar antennas along with matching circuits. A remote user is then placed a distance,  $d$ , from the PhAIA access point and signal strength and throughput can be monitored for different wireless distances and VCSEL bias currents. The effect of long fibre lengths has also been studied in other recent work [1], but here we are looking at unamplified system performance. In this work, a live access point and matching circuits are employed for both uplink and down link PDs. The VCSELs used happen to have input impedances that are almost purely real and close to 50  $\Omega$  at 2.4 GHz [7] and therefore simple matching can be used in this case. The PDs on the other hand are very capacitive in nature and thus the use of lossless matching circuits can remove the resulting mismatch loss and can theoretically improve the link gain by up to 8 dB in both up and down links.

The paper is organized as follows: Section II show results for a basic link. Section III presents the design and performance for lossless matching of the photodiodes. Section IV gives design details of the photonic active integrated antennas. Finally Section V shows the live access point results in infrastructure mode.

Manuscript received April 21, 2008; revised August 15, 2008. First published April 24, 2009; current version published July 09, 2009.

The authors are with the Photonics Research Group, Electrical and Electrical Engineering Department, University of Bristol, Bristol BS8 1UB, U.K. (e-mail: m.cryan@bristol.ac.uk).

Digital Object Identifier 10.1109/JLT.2009.2015587

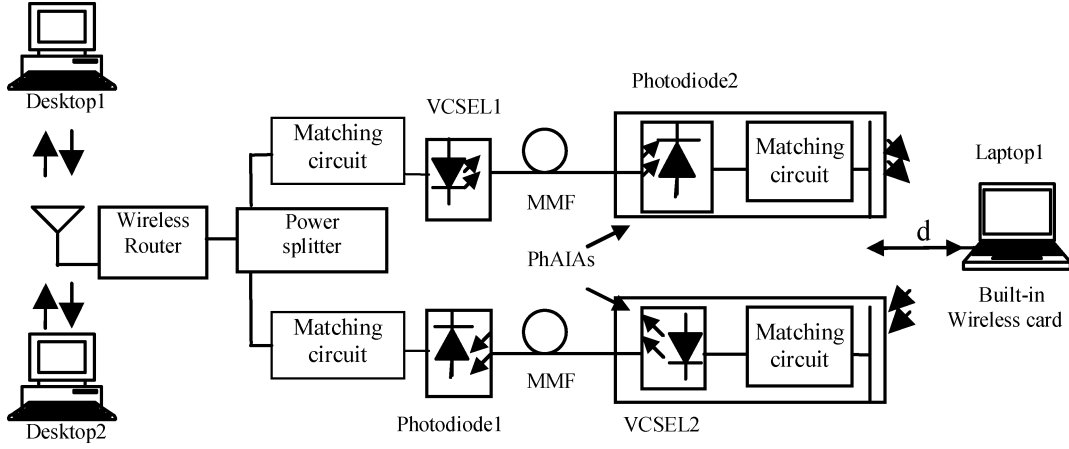


Fig. 1. The WoF concept with matching circuits in infrastructure mode.

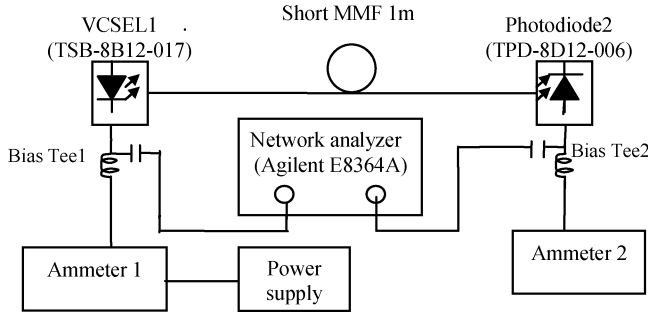


Fig. 2. The basic link diagram.

## II. BASIC LINK CHARACTERIZATION

### A. Link Gain

Two low cost 850 nm VCSELs, (VCSEL1 and VCSEL2) (TSB-8B12-017) from Truelight ([www.truelight.com.tw](http://www.truelight.com.tw)) were used in this work. The slope efficiencies of VCSEL 1 and VCSEL 2 were measured to be 0.40 and 0.42 W/A respectively. In addition, the link consists of two low cost 850 nm GaAs PDs from Truelight (TPD-8D12-006) and their responsivities have been measured to be 0.6 A/W and PD2 to be 0.4 A/W. This difference is due to variations in the coupling from MMF into the PD. The input impedances of the PDs and VCSELs have already been measured in [7].

It is important to initially characterize a short one way link in order to obtain a reference for longer length in-building links and to obtain data for use in the calculation of other link parameters such as noise figure. Therefore, a single VCSEL and PD link was measured using the set up shown in Fig. 2. The measured results are shown in Fig. 3 for different VCSEL1 bias currents.

The results show that a link gain of  $-15$  dB can be achieved at 2.4 GHz. It is useful to confirm that the measured link gain is close to that predicted theoretically. To predict the high frequency link gain is quite challenging [2] and will not be addressed here, the low frequency link gain is more straightforward to predict. When assuming identical source and load impedances in the system, the link gain is given by (1) [7], [11].

$$G = S_L^2 \eta_{lf}^2 T_f^2 \eta_{fd}^2 S_d^2 \frac{R_D}{R_L} \quad (1)$$

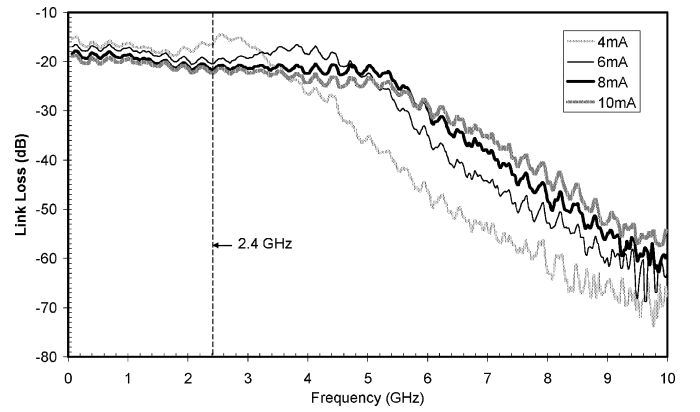


Fig. 3. Link gain at different VCSEL1 bias currents at 2.4 GHz.

where  $S_L$  is the slope efficiency of the laser,  $S_d$  is the responsivity of the PD,  $\eta_{lf}$  and  $\eta_{fd}$  are the coupling efficiencies from laser and PD to MMF respectively,  $R_D$  and  $R_L$  are the impedance of the PD and VCSEL respectively and  $T_f$  is the loss in the fibre.

Since the slope efficiencies are directly measured into the MMF, they can be included together with the coupling efficiency terms and the loss of the short length of MMF is assumed to be negligible. Substituting a VCSEL1 slope efficiency of 0.4 W/A, a PD responsivity of 0.6 A/W,  $R_D \approx 10 \Omega$  and  $R_L \approx 37 \Omega$  (measured VCSEL input resistance [7]), link gain can be calculated to be  $-17.4$  dB. Fig. 3 shows a measured low frequency link gain (at 45 MHz) of between  $-15$  to  $-19$  dB which is close to the calculated value. The variation can be explained by the change in the VCSEL slope efficiency over the range of measured VCSEL bias currents.

### B. Noise Figure of the Link

The noise performance of the link can be expressed in terms of noise figure. The noise figure of an analog link is a measure of the degradation of the signal to noise ratio (SNR) between input and the output of the link. The noise figure,  $NF$ , of the link is defined as [11]

$$NF = 10 \log \left( \frac{\frac{S_i}{N_i}}{\frac{S_o}{N_o}} \right) \quad (2)$$

TABLE I  
NOISE FIGURE AT 2.4 GHz FOR A 1 m MMF LINK

VCSEL current (mA)	Photodiode current (mA)	Link gain $g_i$ (dB)	Noise Figure (dB)
4	0.4	-16	36.10
6	0.7	-20	44.90
8	0.9	-21	48.10
10	1.2	-21	50.56

$$= 10 \log \left( \frac{N_o}{g_i N_i} \right) \quad (3)$$

where  $S_i$  is input signal,  $S_o$  is the output signal,  $N_i$  is input noise power,  $N_o$  is the output noise power and  $g_i$  is the link gain.

The input noise is the thermal noise from a matched resistive load and can be written as [11]

$$N_i = kT\Delta f \quad (4)$$

where  $k$  is Boltzmann's constant which has a value of  $1.38 \times 10^{-23}$  J/K,  $T$  is the measured temperature and  $\Delta f$  is the measurement bandwidth.

The output noise of the link ( $N_o$ ) has three sources which are thermal noise,  $N_{ot}$ , shot noise,  $N_{os}$  and relative intensity noise,  $N_{or}$ . In a 1 Hz bandwidth they can be defined as follows [11]:

$$N_{ot} = g_i kT + N_a \quad (5)$$

$$N_{os} = 2qI_D R_o \quad (6)$$

$$N_{or} = \frac{I_D^2}{2} R_o 10^{RIN/10} \quad (7)$$

where  $q$  is electron charge which has a value of  $1.602 \times 10^{-19}$  C,  $I_D$  is the average photodiode current,  $RIN$  is the laser relative intensity noise in dB,  $R_o$  is the output load resistance and  $N_a$  is the additional noise representing the effects of all the internal link noise sources at the link output.

In this work,  $N_a$  is considered to be the thermal noise of the VCSEL. We can calculate  $N_a$  at the link output in the same way as  $N_i$  which results in an additional  $g_i kT$  term. Substituting (4) – (7) into (3), the expression for the noise figure becomes

$$NF = 10 \log \left( \frac{g_i kT + g_i kT + 2qI_D R_o + \frac{I_D^2 R_o RIN}{2}}{g_i kT} \right) \quad (8)$$

$$= 10 \log \left( 2 + \frac{2qI_D R_o + \left( \frac{I_D^2 R_o RIN}{2} \right)}{g_i kT} \right). \quad (9)$$

Taking  $RIN = -130$  dB provided by the manufacturer,  $R_o = 50 \Omega$ ,  $g_i$  from Fig. 3 at 2.4 GHz,  $T = 290$  K and monitored PD current,  $I_D$ , into (9), the Noise Figure of the basic link for 1 meter of fibre can be calculated as shown in the Table I.

It can be seen that the noise figure can be reduced quite dramatically by decreasing the VCSEL bias current. However, we have to trade this off with the linearity of the link which can be worse at low VCSEL current [7].

In reality much longer fibre links will be used and this will have two competing effects. Firstly there will be decreased link gain and as (9) shows this will lead to increased noise figure. However, the extra fibre loss will reduce the PD current and thus

TABLE II  
NOISE FIGURE AT 2.4 GHz FOR 300 m FIBRE REEL MMF LINK

VCSEL current (mA)	PD current (mA)	Link gain $g_i$ (dB)	Noise Figure (dB)
4	0.18	-35	48.21
6	0.30	-44	61.59
8	0.37	-43	62.40
10	0.50	-42	64.00

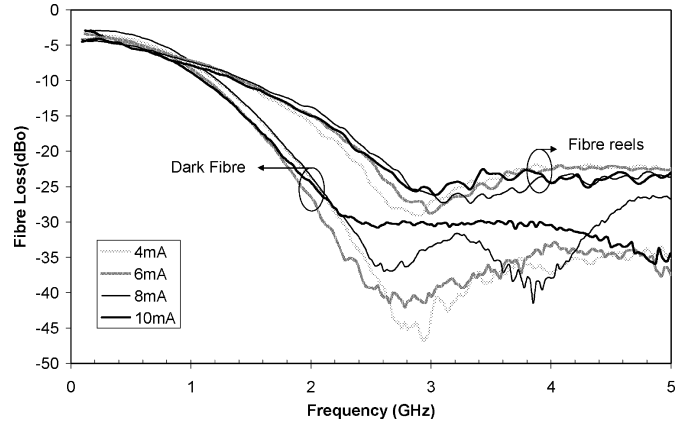


Fig. 4. 634 m in-building and 600 m fibre-reel MMF losses.

reduce both the shot noise and RIN noise as shown in (6) and (7). To quantify these effects a 300 m length has been characterized and the results are shown in Table II.

The results show that longer links have worse noise figure, but for example at 4 mA it is increased by  $\sim 12$  dB, whereas at 6 mA it increases by  $\sim 16$  dB. This highlights the number of parameters which need to be optimized to get good performance in these types of systems.

### C. Multimode Fibre Characterization

Prior to sending data over a link, it is helpful if the fibre being used is characterized in terms of its frequency response. The setup diagram is similar to Fig. 2 but with different fibre lengths, the in-building fibre was looped back on itself to enable VNA measurements to be performed this results in the length of  $2 \times 317 \text{ m} = 634 \text{ m}$ .

In this configuration, the link gain of the 634 m In-building fibre (62.5/125  $\mu\text{m}$ ) was measured and normalized to that of the 1 m MMF link at the same set of VCSEL1 bias currents and is shown in Fig. 4 along with 62.5/125  $\mu\text{m}$  fibre-reel MMF links of a similar length 600 m.

The results show that there is a large amount of extra loss associated with the in-building fibre. There are a number of possible reasons for this difference, firstly, the in-building fibre could have a number of very tight bends which will alter the differential mode delay (DMD) of the fibre and hence affect the frequency response. Secondly, MMFs which are nominally identical can have very different frequency responses due to fabrication imperfections.

The results also show that the RF fibre loss is not constant with VCSEL bias current and with appropriate choice of bias the loss at working frequency of 2.4 GHz can be improved

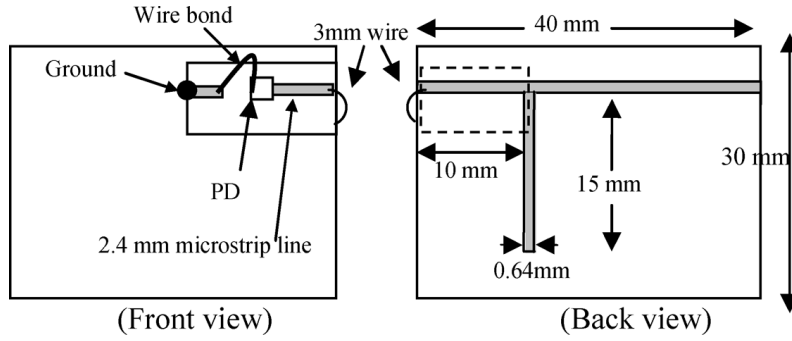


Fig. 5. Layout of the PD on the microstrip carrier with matching circuit.

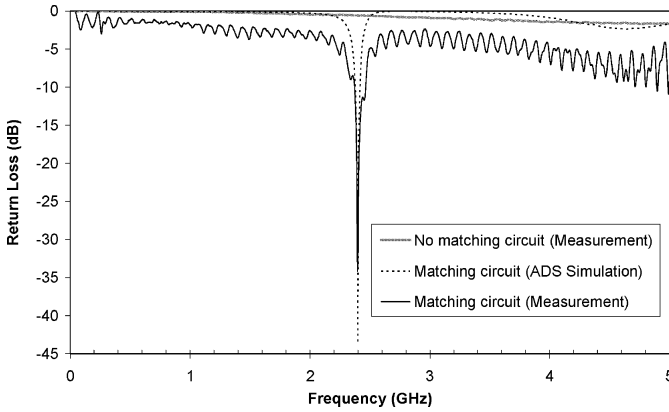


Fig. 6. The measured and modelled return loss of the PD with and without (measured only) matching.

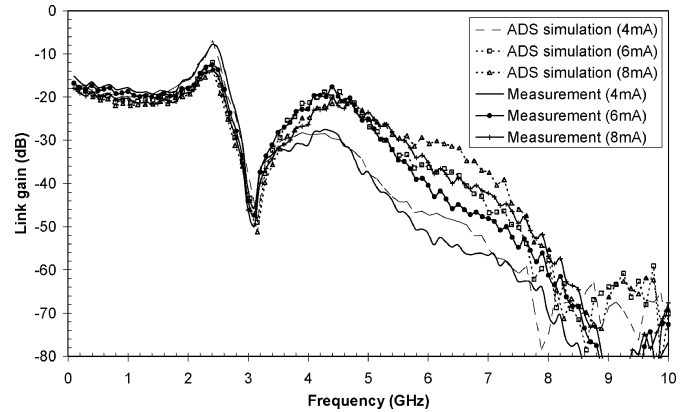


Fig. 7. The simulated and measured link gain for the basic link versus VCSEL bias current.

by 10 dB. This has been observed previously [12], [13] and is caused by the VCSEL beam spot and therefore launch position offset changing as a function of the VCSEL current.

### III. LOSSLESS MATCHING CIRCUITS IN THE BASIC LINK

#### A. Matching Circuit Modeling

Initially simple single stub has been used and the design has been implemented using Agilent's Advanced Design System (ADS). For low cost implementation the matching circuit and optical device mounting circuit would be implemented on the same PCB, however, for ease of prototyping, this has not been implemented here. Thus two PCBs are used, one with a built-in via hole which carries the optical chip (microstrip carrier) and one which implements the matching circuit. Since both boards need the same ground plane the two boards are placed back-to-back. This also enables easy alignment of the fibre to the optical devices, whilst allowing access to the matching circuit for fine tuning. A connection between the microstrip lines on the two boards is achieved with 3 mm long wire, the inductance of which is included in the matching circuit. The input impedance of the PD is measured as  $Z_{pd} = 10 - j100 \Omega$  at 2.4 GHz [7] and for matching purposes this is represented as a model of  $10 \Omega$  series resistor and capacitor,  $C_D = 0.663$  pF. The PD circuit model at 2.4 GHz and a single stub matching is designed on ADS on low loss substrate ( $\epsilon_r = 4$ , thickness = 0.33 mm). The results for this are shown in Fig. 6, where very good matching is seen at 2.4 GHz.

The matching circuit was fabricated and was then fine tuned by altering the dimensions of the strip lines by adding copper tape. The new matching circuit can be seen in Fig. 5, the length of the stub has been increased from 14.14 mm as designed to 15 mm. The results are shown in Fig. 6 and it can be seen that very good matching is achieved.

#### B. Link Gain Improvement Using Lossless Matching Circuit

In order to confirm the improvement in link gain obtained by matching, the simple link was remeasured this time including the PD matching circuit. This setup is similar to Fig. 2 except for PD matching circuit included with results shown in Fig. 7.

Fig. 7 shows a measured peak link gain of  $-5$  dB at 2.4 GHz which is increased by 11 dB from the unmatched case. The mismatch loss ( $L_M$ ) which is being removed by matching can be defined by

$$L_M(\text{dB}) = 10 \log(1 - |\rho_L|^2). \quad (10)$$

where  $\rho_L$ , the reflection coefficient of the PD, is given by

$$\rho_L = \frac{Z_L - R_0}{Z_L + R_0}. \quad (11)$$

Substituting PD impedance ( $10 - j100 \Omega$ ) and load impedance ( $50 \Omega$ ) in the (10) and (11), we can calculate the mismatch loss to be 8.33 dB which is close to the measured improvement. The discrepancy here will be due partly to the accuracy of the measurement of the PD input impedance and also to alignment repeatability between these two sets of measurements. There is a

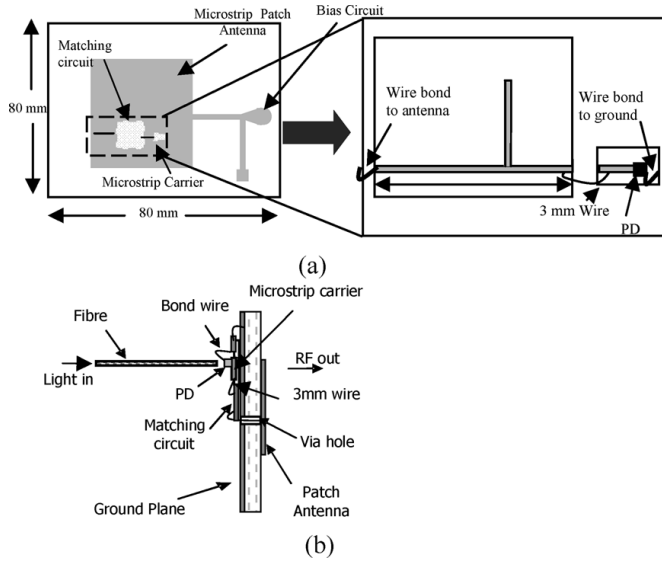


Fig. 8. The configuration of PhAIAs with PD: (a) front view showing layout of microstrip patch, bias network, matching circuit and photonic device carrier mounted on the reverse side, (b) side view.

large dip in the link gain at 3 GHz, to fully understand this, an ADS model of the link gain has been developed which is described below.

### C. Matched Link Gain Simulation on ADS

Analysis of matched links has been carried out previously [14], [15], however, the approach was only valid at a single resonant frequency and this might be not sufficient in some applications such as wideband systems and practical links which are normally lossy. Thus, in this paper, we propose to use measured 2-port link S-parameters which can be imported into a S2P datablock within ADS. The model includes an ideal transmission line to de-embed the effects of the microstrip carrier, coaxial cable and SMA connector. The effect of the 3 mm wire was represented by 2 nH inductor. Fig. 7 shows the results and it can be seen that the large dip is being modeled very well. The dip is caused by the stub acting as a short circuit at this particular frequency. It can also be seen that there is very good agreement between the simulation and measurement results at the same VCSEL1 bias current. Not only at the resonant frequency but also the whole frequency range from 0.04 to 10 GHz. This modeling approach would therefore allow dual band or wide band matching circuits to be developed in a straightforward manner.

## IV. PHOTONIC ACTIVE INTEGRATED ANTENNAS

This section applies the PhAIA concept where the VCSELs and PDs are integrated on the rear of the patch antennas. Unlike the PD, the measured input impedance of VCSEL is already close to  $50 \Omega$ , therefore, the PhAIA with VCSEL does not require any modification from [7]. In this section, we will only focus on the PhAIA with matched PD. Fig. 8 shows front and side views of the PhAIA with matched PD.

This configuration resembles that shown in [7] but the matching circuit is now included. The antenna is designed on FR4 ( $\epsilon_r = 4.5$ , thickness = 1.5 mm) to operate at 2.4 GHz. A

microstrip carrier and the matching circuit as shown in Fig. 5 are now mounted and soldered on to the rear of the antenna forming a single ground plane. The output of the matching circuit is then carefully connected to the  $50 \Omega$  position of the non-radiating edge of the antenna. The PD is used in short circuit mode and thus a closed loop is required to allow the photocurrent to flow. The bias circuit and the patch antenna form part of this loop and the bias circuit prevent the RF signals from flowing around this loop.

## V. BI-DIRECTIONAL WoF LINK USING A LIVE ACCESS POINT

This section shows a potential commercial scenario whereby WiFi coverage within a building can be improved without altering the number of access points. This approach competes against the costs of installing and wiring up a new access point or installing a wireless repeater. The WoF approach also allows the WiFi signals be transmitted many 100's of meters beyond the normal 100 m limit of standard copper twisted pair. In certain scenarios this could remove the requirement for the installation of a complete router cabinet. However, to be commercially competitive against incumbent technologies, the costs of the WoF approach must be very low and the use of PhAIAs and low cost VCSELs and PDs will help to achieve this.

To perform the test the project was granted access to the University of Bristol's WiFi network and was allocated a specific SSID such that connections to the specific access point could be confirmed amongst the myriad of WiFi signals that are found in urban environments such as this. In order to connect to the access point the in-building fibre links had to be reconfigured which resulted in a length of 317 m. The setup diagram can be seen in Fig. 9.

Since the access point operates in switched diversity mode [16] this configuration allows the remote laptop2 to share access to the internet with a local user, laptop1. In order to tap off the signal from the access point (Cisco Aironet 1200 series), one of the 2.4 GHz external antennas was removed and directly fed to the coaxial cable to the power splitter.

The tapped-off signal, is measured coaxially by an RF spectrum analyzer (Anritsu MS2668) using the peak hold feature which allows the full signal spectrum to be captured and is found to be 0 dBm This is somewhat lower than expected and could be due to settings at the access point over which we currently have no control. This signal is fed into the splitter and then into the non-antenna transmitter and receiver. This results in an input power to the transmitter of approximately  $-10$  dBm. At the laptop2 side, the distance between the PhAIAs and the laptop,  $d$  was varied from 0.1 to 4.5 m. The results for throughput and signal strength as a function of  $d$  and VCSEL1 bias current are shown in Figs. 10 and 11 both with and without the use of PD matching circuits. A minimum distance of 0.1 m has been used here, however this would not be used in a practical system. In reality there would be a minimum distance of 1–2 m and thus the inclusion of extra amplification at both the local and remote ends could improve the maximum distance well beyond the 4 m limit shown here. Care would have to be taken not to saturate the local end VCSEL whereby linearity effects would decrease the system performance. Also the inclusion of amplification at the remote end would significantly increase the DC

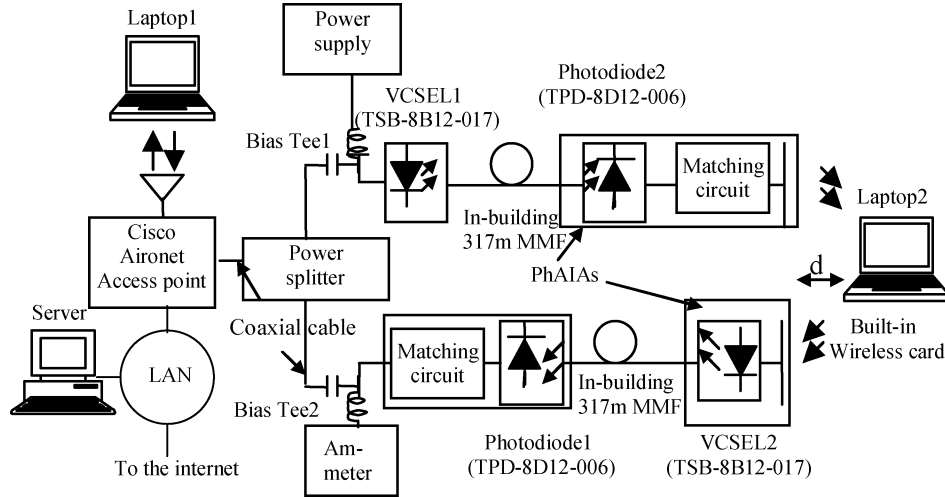


Fig. 9. The bi-directional WoF link setup including matching circuits.

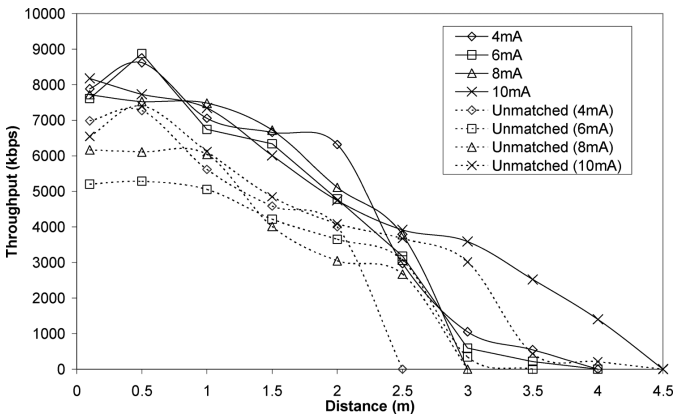


Fig. 10. Throughput versus distance at different VCSEL1 bias current.

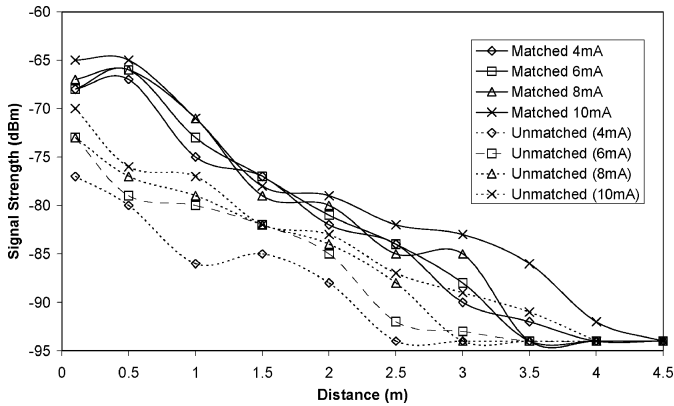


Fig. 11. Signal strength versus distance at different VCSEL 1 bias current.

power budget making power-over-fibre based operation more difficult to achieve.

During the test, the VCSEL2 bias current was set to 6 mA and the sensitivity of the built-in laptop2 wireless adapter (Intel PRO Wireless 3945ABG) was found from the datasheet to be  $-95$  dBm at 1 Mbps. Proprietary software provided by Provision Communications was used to measure the throughput of the downlink to laptop2 and the signal strength software Wi-fi

TABLE III  
RF DOWNLINK BUDGET AT 1 m

VCSEL1 current (mA)	Input Power at VCSEL1 (dBm)	Link Gain (dB) Matched	Output Power at PD2 (dBm) Matched	Free Space Loss at 1m (dB)	Received Power at Laptop (dBm)
4	-10	-27	-37	33	-70
6	-10	-30	-40	33	-73
8	-10	-30	-40	33	-73
10	-10	-29	-39	33	-72

sistr ([www.dnsoft.be](http://www.dnsoft.be)) was used to measure the signal strength. Fig. 10 illustrates that the throughput for the matched case can be maintained up to 7 Mbps over 2 m and almost 1 Mbps over 4 m while the throughputs for non matching are significantly lower at the same distance. This is consistent with the signal strength in Fig. 11 that the signal strength of unmatched system is typically 10 dB lower than the matched case.

Ideally the throughput should be maintained close to the level available from the original access point  $\sim 10$  Mbps. In order to achieve this Figs. 10 and 11 show that the received signal strength needs be greater than  $-70$  dBm. It is useful to look at the link budget to understand what improvements are required to achieve this. Table III shows this for the downlink for different VCSEL1 bias currents including the effects of free space loss. This uses the well-known path loss equation from the Keenan-Motley propagation model defined in (12) [2]

$$PL(\text{dB}) = G_1 + G_2 + 10 \log \left( \frac{4\pi f}{c} \right)^2 d^n \quad (12)$$

where  $f$  is the frequency,  $c$  is the velocity of light,  $n$  is the path loss exponent which has a value from 3 to 4 for indoor environment and  $G_1$  and  $G_2$  are the gains of the PhAIA and laptop antennas. Taking  $f = 2.4$  GHz,  $d = 1$  m,  $c = 3 \times 10^8$  m/s and  $n = 3$ , and typical gain values for the antennas of  $G_1 = +7$  dBi and  $G_2 = 0$  dBi (isotropic), the path loss can be calculated. Table III shows good agreement with measured data in Fig. 11. Thus for example by including a 15 dB gain amplifier at the local end of the link the throughput at 4 m could be increased

TABLE IV  
RF UPLINK BUDGET AT 1 m

VCSEL2 current (mA)	Input Power at VCSEL2 (dBm)	Link Gain (dB) Matched	Output Power at PD2 (dBm) Matched	Cable & Splitter losses (dB)	Received Power at Access point (dB)
4	-37	-27	-64	10	-74
6	-37	-30	-67	10	-77
8	-37	-30	-67	10	-77
10	-37	-29	-66	10	-76

to around 8 Mbps. This assumes there are no adverse effects on linearity. An alternative is to increase the  $-10$  dBm input power. Both of these scenarios are now being explored and will be detailed in future work.

It is useful to calculate the RF link budget for the uplink as well as downlink in order to understand which link is limiting the system performance. Unfortunately, the software being used here was unable to measure the uplink throughput and signal strength. Therefore, an RF spectrum analyzer (Anritsu MS2668) and patch antenna designed as shown in Fig. 8 was used to measure the output power from the laptop at a distance of 1 m. The received power here is approximately the same as the input power at VCSEL2. Assuming the link gain of the uplink and downlink are identical, we can calculate the uplink budget as can be seen in Table IV.

Table IV shows the received power at the access point when placing the laptop 1 m away from the patch antenna. This information together with the sensitivities of the laptop and access point can be used to determine whether the system is uplink or downlink limited. Taking the sensitivity of the access point to be  $-94$  dBm and the laptop to be  $-95$  dBm at 1 Mbps, the downlink and uplink received signals at a VCSEL bias current of 10 mA are 23 and 18 dB above the respective sensitivities and thus the system is being uplink limited.

## VI. CONCLUSION

This paper has presented the use of low cost PhAIAs to implement low cost WiFi links in infrastructure mode. The paper starts from the basic link gain and NF calculation and then shows how lossless matching can be used to theoretically improve the link gain by more than 8 dB. This approach has been used in a live trial in the University of Bristol WiFi network showing a potential commercial scenario where WiFi coverage within a building can be extended by many 100's of meters. Here legacy fibre has been used, but provided the costs are low enough this may be an attractive option even with newly installed fibre which could be either single mode or multimode. In the longer term complete systems based on these ideas could be installed which could dramatically simplify WLAN management and reduce costs. Further system developments are now under way in order to reduce costs and improve the RF range and throughput. These include the use of amplifiers and alternatives to simple splitters such as circulators and Wilkinson dividers. This will allow the WoF approach to become even more competitive against the more conventional approaches using wireless repeaters or installation of more

access points to improve in-building WiFi coverage. It should also be pointed out that the WoF approach outlined here can be used over wide bandwidths by employing wideband matching techniques and multiband antennas. Thus it has the potential to distribute 3G, UMTS, and UWB signals simultaneously, though this can require much higher performance in terms of linearity.

## ACKNOWLEDGMENT

The authors would like to thank Prof. D. Bull of Provision Communications and P. Ferre for providing the throughput measurement codes, S. Shahin for help with the in-building fibre connections and J. Hooper and H. Glogowski for granting access UoB WiFi access point and network.

V. Sittakul would like to acknowledge the Royal Thai Government Scholarship for Ph.D. funding.

## REFERENCES

- [1] A. Das, M. Mjeku, A. Nkansah, and N. J. Gomes, "Effects on IEEE 802.11 MAC throughput in wireless LAN over fiber systems," *IEEE J. Lightw. Technol.*, vol. 25, no. 11, pp. 3321–3328, Nov. 2007.
- [2] A. Das, A. Nkansah, N. J. Gomes, J. C. Batchelor, and D. Wake, "Design of low-cost multimode fiber-fed indoor wireless networks," *IEEE Trans. Microw. Theory Tech.*, vol. 54, no. 8, pp. 3426–3432, Aug. 2006.
- [3] T. Niiho, M. Nakaso, K. Masuda, H. Sasai, K. Utsumi, and M. Fuse, "Transmission performance of multichannel wireless LAN system based on radio-over-fiber techniques," *IEEE Trans. Microw. Theory Tech.*, vol. 54, pp. 980–989, Feb. 2006.
- [4] P. K. Tang, L. C. Ong, A. Alphones, B. Luo, and M. Fujise, "PER and EVM measurements of a radio-over-fiber network for cellular and WLAN system applications," *IEEE J. Lightw. Technol.*, vol. 22, no. 11, pp. 2370–2376, Nov. 2004.
- [5] M. Sauer, A. Kobayakov, and J. George, "Radio over fiber for picocellular network architectures," *IEEE J. Lightw. Technol.*, vol. 25, no. 11, pp. 3301–3320, Nov. 2007.
- [6] M. J. Crisp, L. Sheng, A. Watts, R. V. Penty, and I. H. White, "Uplink and downlink coverage improvements of 802.11g signals using a distributed antenna network," *IEEE J. Lightw. Technol.*, vol. 25, no. 11, pp. 3388–3389, Nov. 2007.
- [7] V. Sittakul and M. J. Cryan, "A fully bidirectional 2.4 GHz wireless-over-fiber system using photonic active integrated antenna (PhAIAs)," *IEEE J. Lightw. Technol.*, vol. 25, no. 11, pp. 3358–3365, Nov. 2007.
- [8] L. Noel, D. Wake, D. G. Moodie, D. D. Marcenac, L. D. Westbrook, and D. Nasset, "Novel techniques for high-capacity 60-GHz fiber-radio transmission systems," *IEEE Trans. Microw. Theory Tech.*, vol. 45, pp. 1416–1423, Aug. 1997.
- [9] M. J. Cryan, M. Dragas, J. Kung, V. Jain, F. Fornetti, T. Houle, R. M. J. Varrazza, and M. Hill, "A 2.4-GHz wireless-over-fiber transceiver using photonic active integrated antennas (PhAIAs)," *Microw. Opt. Technol. Lett.*, vol. 48, no. 2, pp. 233–237, Dec. 2005.
- [10] J. G. Werthen and M. Cohen, "Photonic power: Delivering power over fiber for optical networks," in *Proc. Photonics in Switching Int. Conf.*, Oct. 2006, pp. 1–3.
- [11] C. H. Cox, III, *Analog Optical Links Theory and Practice*. Cambridge, U.K.: Cambridge Univ. Press, 2002.
- [12] C. Xia and W. Rosenkrunz, "Statistical analysis of electrical equalization of differential mode delay in MMF links for 10-Gigabit ethernet," in *Proc. OFC/NFOEC*, Mar. 6–11, 2005, vol. 5, p. 3.
- [13] L. Raddatz, I. H. White, D. G. Cunningham, and M. C. Nowell, "An experimental and theoretical study of the offset launch technique for the enhancement of the bandwidth of multimode fiber links," *IEEE J. Lightw. Technol.*, vol. 16, no. 3, pp. 324–325, Mar. 1998.
- [14] J. J. Gulick *et al.*, "Fundamental gain/bandwidth limitations in high frequency fiber-optic links," in *Proc. SPIE High Frequency Opt. Commun.*, Sep. 1986, vol. 716, pp. 76–81.
- [15] M. L. Chapelle, J. Gulick, and H. P. Hsu, "Analysis of low loss impedance matched fiber-optic transceivers for microwave signal transmission," in *Proc. SPIE*, Sep. 1986, vol. 716, pp. 120–125.
- [16] Cisco Aironet 1200 Series Datasheet, [Online]. Available: www.cisco.com





**Vitawat Sittakul** (S'08) was born in Bangkok, Thailand, in March 1979. He received the B.Eng. degree in telecommunication from Chulalongkorn University, Bangkok, Thailand, in 2000 and the M.Sc. degree (with distinction) in optical and communication systems from Northumbria University, Newcastle, U.K., in 2003. He has been working toward the Ph.D. degree at the University of Bristol, Bristol, U.K., since 2006.

From 2003 to 2004, he was a Measurement Engineer with Fabinet, where he was a global engineering- and manufacturing services provider. From 2004 to 2006, he was a Senior RF Engineer with Advance Information Service Company, Ltd., which is the biggest mobile service provider in Bangkok. His research interest is in radio-over-fiber.



**Martin J. Cryan** (S'91–M'95–SM'01) received the B.Eng. degree in electronic engineering from The University of Leeds, Leeds, U.K., in 1986, and the Ph.D. degree from the University of Bath, Bath, U.K., in 1995.

He was a Microwave Design Engineer for five years following his undergraduate studies. From 1994 to 1997, he was a Researcher with the University of Birmingham, where he worked on active integrated antennas. From 1997 to 1999, he was a European Union Training and Mobility of Researchers Research Fellow working at the University of Perugia, Perugia, Italy, on the design and simulation of quasi-optical multipliers using the lumped-element FDTD method. From 2000 to 2002, he was a Research Associate at the University of Bristol, Bristol, U.K., working on hybrid electromagnetic methods for EMC problems in optical transceivers and FDTD analysis of photonic crystals. In 2002, he became a Lecturer in the Department of Electrical and Electronic Engineering, University of Bristol, and was made Senior Lecturer in 2007. He has published 35 journal and more than 100 conference papers (eight invited), in the areas of fabrication, modeling and measurement of photonic crystal based devices, radio-over-fibre, active integrated antennas, FDTD analysis and MMIC design.